Article

Dissolution of CaO in SiO$_2$-CaO-Al$_2$O$_3$ Slag in Si Production

Marit Buhaug Folstad *, Kristian Etienne Einarsrud [ID] **and Merete Tangstad** [ID]

Department of Materials Science and Engineering, Norwegian University of Science and Technology,
7034 Trondheim, Norway; kristian.e.einarsrud@ntnu.no (K.E.E.); merete.tangstad@ntnu.no (M.T.)
* Correspondence: marit.b.folstad@ntnu.no

Abstract: This work investigates the dissolution of CaO into three different compositions of SiO$_2$-CaO-Al$_2$O$_3$ slag similar to those found in industrial Si furnaces. It was found that CaO dissolution into the slag is fast. During the dissolution process, a layer containing 35–42% CaO was formed between the CaO particle and the slag, which corresponded to the phases CaO·Al$_2$O$_3$·2SiO$_2$ or 2CaO·Al$_2$O$_3$·SiO$_2$ in this study. Two models were investigated to determine the dissolution rate of the three slags. In the first model, the CaO particle is assumed to be a smooth shrinking sphere, and the rate controlled by the chemical reaction rate. The second model assumes that the rate is controlled by mass transport and depends on the diffusion rate of CaO through a boundary layer on the surface of the CaO. Both models gave similar accuracy to the experimental values, and a proportional relationship between the rate constants and the viscosities was obtained. At 1500 °C, the diffusion coefficients were found to be in the order of 10^{-6} cm^2/s.

Keywords: CaO; slag; viscosity; dissolution; dissolution rate; shrinking sphere; mass transport model; silicon production

1. Introduction

Metallurgical silicon (Si) is produced industrially by carbothermic reduction of quartz (SiO$_2$) in a submerged arc furnace. The overall mass balance can be written as in reaction 1, but the actual process is more complex and happens in several steps. In the furnace, there are also several oxide impurities present as slag.

$$SiO_{2\,(s)} + 2C_{(s)} = Si_{(l)} + 2CO_{(g)} \qquad (1)$$

The Si furnace is normally divided into a low-temperature zone, which includes the higher parts of the furnace and along the furnace walls, and a high-temperature zone in the lower parts of the furnace around the electrode tip [1]. Based on COMSOL simulations, Myrhaug [2] made a conceptual model of the temperature profile and Si flow in the Si furnace. Figure 1 shows an illustration of a Si furnace, including the main zones and approximate temperatures at different positions. The highest temperatures can be found right below the electrodes, around the arc. Below the cavity is the metal bath, which holds a temperature around 1900–2000 °C. With increasing distance from the arc, upwards in the furnace and towards the furnace lining, the temperature decreases. According to calculations, the temperature ranges from around 1000 °C to 1500 °C above the tap-hole and in the slag/inactive zone. The slag in the furnace will therefore experience different temperatures, depending on where it is located.

Experimental research has found that the mass transfer in the slag is typically the rate-determining step for the CaO dissolution in SiO$_2$-CaO-Al$_2$O$_3$ slag. A number of researchers have also deduced the diffusivity from dissolution rate data [3–11]. A short summary with the diffusion coefficients together with the respective slag composition and temperature is listed in Table 1. The chemical and physical properties in the slag are important factors when describing the rate of dissolution reactions in oxides.
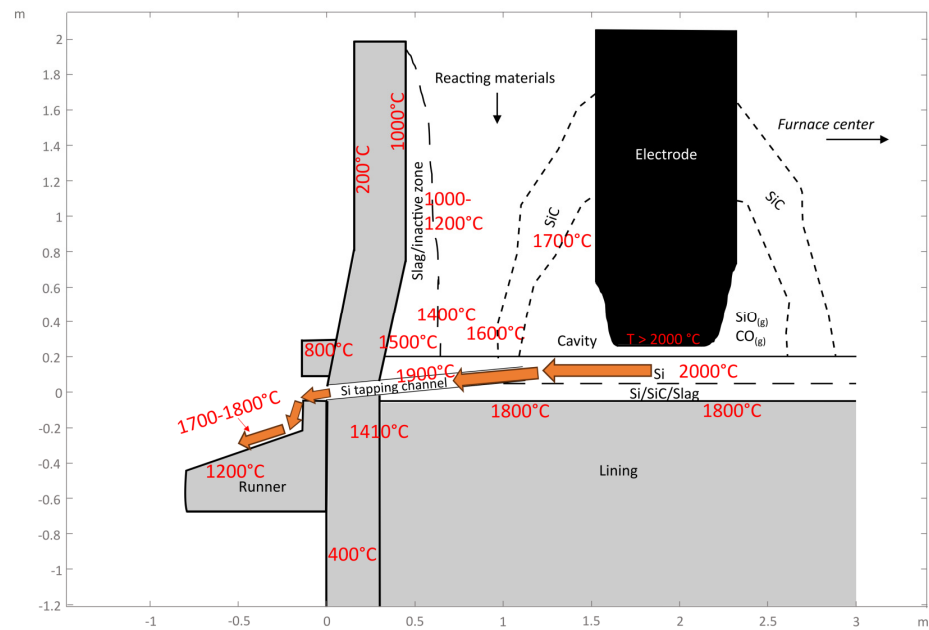
Figure 1. Illustration of a Si furnace including the main zones and approximate temperatures at different positions. The temperatures are based on modeled temperatures from Myrhaug [2].

Table 1. Summary of earlier research on the dissolution of CaO in SiO_2-CaO-Al_2O_3 slag. D is the diffusion coefficient.

Authors	Slag Composition			Temperature	D	Comment
	SiO_2 [wt%]	CaO	Al_2O_3	[°C]	[cm²/s]	
Towers et al. [3] (1953)	40	40	20	1450	$1 \times 3 \times 10^{-6}$	Radioactive Tracer Technique, Ca^{45}
Towers and Chipman [4] (1957)	40	39	21	1430	1×10^{-6}	Radioactive Tracer Technique, Ca^{45}
				1350	3.3×10^{-7}	
	40	40	20	1400	6.2×10^{-7}	
				1450	1.3×10^{-7}	
Niwa [5] (1957)				1350	5.2×10^{-7}	Radioactive Tracer Technique, Ca^{45}
	39	43	18	1400	6.4×10^{-7}	
				1450	9.5×10^{-7}	
	71	11	18	1350	0.39×10^{-7}	
				1400	3.2×10^{-7}	
	41	40	19	1350	3.9×10^{-7}	
				1395	6.9×0^{-7}	
				1440	10×10^{-7}	
	37	43	20	1440	8×10^{-7}	
				1510	10×10^{-7}	
	39	49	12	1440	11.5×10^{-7}	
				1510	17×10^{-7}	
Saitô and Maruya [6] (1958)	36	45	19	1510	8.5×10^{-7}	Semi-infinite medium, Ca^{45}
				1530	9.9×10^{-7}	
				1440	3.8×10^{-7}	
				1485	7.1×10^{-7}	
	34	46	20	1510	8.4×10^{-7}	
				1530	10.3×10^{-7}	
				1575	13.0×10^{-7}	
	31	48	20	1540	5.5×10^{-7}	
				1565	8.1×10^{-7}	
				1400	9.2×10^{-7}	
Goto et al. [7] (1977)	40	40	20	1450	1.6×10^{-6}	Calculated values from Nernst–Einstein relation
				1500	2.6×10^{-6}	

Table 1. *Cont.*

Authors	Slag Composition SiO₂ [wt%]	CaO	Al₂O₃	Temperature [°C]	D [cm²/s]	Comment
Liang et al. [8] (1996)	60	30	10		7.41×10^{-7}	
	55	25	20		5.18×10^{-7}	
	65	20	15		3.3×10^{-7}	
	65	25	10		4.78×10^{-7}	
	55	30	15	1500	7.12×10^{-7}	Isotope tracer method, Ca^{40} and Ca^{42}
	60	20	20		3.66×10^{-7}	
	60	25	15		4.5×10^{-7}	
	45	35	20		9.32×10^{-7}	
	40	40	20		1.34×10^{-6}	
Amini et al. [9] (2006)	8	50	42	1500–1600	In the range 10^{-5}–10^{-4}	Calculated from forced convection dissolution rate data using known mass-transfer correlations
Zhang and Chou [10] (2011)	40	40	20	1350	9.0×10^{-7}	Calculated values from Nernst–Einstein relation
				1400	1.3×10^{-7}	
				1450	1.9×10^{-7}	
				1500	2.8×10^{-7}	
Ren et al. [11] (2013)	25	46	29	1350	3.74×10^{-7}	Model from relation between diffusion activation energy and optical basicity
				1395	6.13×10^{-7}	
				1440	9.8×10^{-7}	
	27	49	24	1440	8.80×10^{-7}	
				1510	18.90×10^{-7}	
	45	45	10	1350	3.14×10^{-7}	
				1400	5.72×10^{-7}	
				1450	10.6×10^{-7}	
	44	47	9	1350	8.39×10^{-7}	
				1400	11.43×10^{-7}	
				1450	15.28×10^{-7}	
	25	49	26	1350	2.64×10^{-7}	
				1500	16.67×10^{-7}	
				1540	25.88×10^{-7}	

The first studies on the diffusion process of the Ca ion into SiO_2-CaO-Al_2O_3 slag were conducted by using the radioactive tracer technique and the capillary method [3–5]. The results suggested that the diffusion coefficient for Ca diffusion in ~40 wt% SiO_2—40 wt% CaO—20 wt% Al_2O_3 is in the range of 10^{-7}–10^{-6} cm²/s in the temperature range of 1350–1550 °C. Saitô and Maruya [6] used the semi-infinite medium method in the temperature range 1350–1600 °C to measure the self-diffusion coefficients of calcium in several compositions of molten SiO_2-CaO-Al_2O_3 slags. The diffusion coefficients were found to be in the order of 10^{-6}–10^{-7} cm²/s.

Goto et al. [7] calculated diffusion coefficients for 40 wt% SiO_2—40 wt% CaO—20 wt% Al_2O_3 slag in the temperature interval 1350–1500 °C based on Nernst–Einstein relation. The purpose was to examine its validity on multi-component oxide slags. For this, they compared with experimental data from Towers et al. [3,4], Niwa [5] and Saitô and Maruya [6]. Zhang and Chou [10] used the same method to estimate the diffusion coefficient of calcium ions in the same slag and a temperature interval of 1350–1500 °C. For both Goto et al. and Zhang and Chou, the calculated results were larger than the experimental values.

Liang et al. [8] measured the diffusion coefficient of Ca^{40} and Ca^{42} at 1500 °C and 1 GPa for several slag compositions using the isotope tracer method. Their results for 40 wt% SiO_2—40 wt% CaO—20 wt% Al_2O_3 are similar as the results from Towers and Chipman [4]. They also found that the self-diffusion coefficient increased with decreasing viscosity of the slag, i.e., with decreasing SiO_2 and Al_2O_3 content in the slag. However, they did not follow the Stokes–Einstein equation or the Eyring equation. The Eyring equation, shown in Equation (2), has often been used to relate melt viscosities with diffusion coefficients [12]:

$$D = \frac{kT}{\eta \lambda} \tag{2}$$

where k is Boltzmann constant, T is the temperature, η is the viscosity and λ is the mean interatomic difference.

Eyring et al. [13] suggested that the driving force for diffusion resulted from the concentration gradient of diffusion ions, and that the standard free energy changed with the jumping distance. The structure and physical properties of molten slags may then change with the increasing content of CaO, which again changes the jumping distance of Ca-ion and the value of the diffusion activation energy. Self-diffusion coefficients of alkali and alkaline earth elements in molten silicates, however, did not follow this simple relation, which was also supported by [14–16].

The diffusion coefficient is strongly influenced by the viscosity of the slag. The viscosity of a slag is the resistance to flow of one layer of molecules over another and depends on composition and temperature. The viscosity will affect the mass transfer of ions between the CaO and slag interface, and through the liquid slag. Dogan et al. [17] found in their study that with increasing slag density, the viscosity decreased and the diffusivity of slag in SiO_2-CaO-FeO increased. This means that the slag structure is an important factor for the diffusion of CaO in slag.

Ren et al. [11] developed a model for estimating the diffusion coefficient related to the structure of the slag instead of viscosity and electrical conductivity. The structure of the slag is often described by optical basicity, free oxygen, bridging oxygen, non-bridging oxygen and the ratio of non-bridging oxygen to tetrahedral cations. The optical basicity was used to both describe the structure of the slag and to estimate its physical properties. They used Equation (3) from Mills [18] for optical basicity that accounts for the cations required for the charge balance of AlO_4^{5-}. The valence of Al^{3+} is lower than Si^{4+}, so Ca^{2+} is needed to keep the charge balance and forms $[½Ca(AlO_4)]^{4-}$.

$$\Lambda^{corr} = \frac{1.0(\chi_{CaO} - \chi_{Al_2O_3}) + 0.6 \times 3\chi_{Al_2O_3} + 0.48 \times 2\chi_{SiO_2}}{(\chi_{CaO} - \chi_{Al_2O_3}) + 3\chi_{Al_2O_3} + 2\chi_{SiO_2}} \tag{3}$$

where Λ^{corr} is the corrected optical basicity, x_i is the mole fraction of each component, and the coefficients 1.0, 0.6 and 0.48 are the optical basicities of CaO, Al_2O_3 and SiO_2, respectively.

Next, they plotted Λ^{corr} as a function, as shown in Equation (4), and found the approximate relation, as in Equation (5):

$$B = \frac{E}{R} \tag{4}$$

$$B = a\Lambda^{corr3} + b\Lambda^{corr2} + c\Lambda^{corr} + d \tag{5}$$

where E is the activation energy and R is the universal gas constant (8.314 J/K mol). The constants a, b, c and d were optimized by using experimental data from Goto et al. [7] and Zhang and Chou [10]. In the model from Ren et al. [11], there was an increasing function relationship between the logarithm of the pre-exponential factor and the diffusion activation energy calculated by optical basicity. With the increasing polymerization degree of molten slag, the diffusion coefficient of calcium ions decreases. They explained that a decreasing concentration of free Ca^{2+} and weaker mobility of these calcium ions in $[1/2Ca(AlO_4)]^{4-}$ resulted in a lower diffusion coefficient because of the charge balance in the $CaO–Al_2O_3–SiO_2$ slag. The diffusion coefficients were calculated to be in the range of $10^{-7}–10^{-6}$ cm^2/s, and the activation energy was calculated to be about 140–320 kJ/mol.

Amini et al. [9] calculated the diffusivity of lime in 8 wt% SiO_2—50 wt% CaO—42 wt% Al_2O_3 slag from experimental results on the dissolution rate in the temperature interval 1500–1600 °C. A rotating disc was used during the dissolution rate experiments, and they calculated the diffusion coefficient via the total mass flux. They found that the diffusion coefficient was in the range of 10^{-4} cm^2/s. As the diffusion coefficient was calculated from dissolution data under forced convection, it is expected to give a higher value than

for self-diffusion. They also looked at the effect of adding 5 wt% SiO_2 to the slag, which decreased the CaO diffusivity.

CaO, in the form of limestone ($CaCO_3$), is often added as a flux in Si production. Its purpose is to reduce the viscosity of the slag and thereby prevent accumulation. Too much accumulated slag is negative for furnace operation. Therefore, the dissolution rate of CaO into SiO_2-CaO-Al_2O_3 slag plays an important role on the slag properties in the furnace and it is of interest to investigate the kinetics of this process. The main goal of this study is to investigate the effect of dissolving CaO in SiO_2-CaO-Al_2O_3 slag compositions relevant for the Si production. A lot of research has been conducted on this reaction, but the research is related to the steel industry with slag compositions around 40 wt% SiO_2—40 wt% CaO—20 wt% Al_2O_3. The CaO content in the Si furnaces is lower, around 10–20%. A lower CaO content increases the driving force of CaO mass transfer in the slag and hence also increases the reaction rate. Dissolution experiments with slag compositions similar to those found in Si furnaces were conducted in this study.

2. Materials, Equipment and Methods

Based on slag compositions found in accumulated slag samples in industrial Si furnaces [19,20], three different compositions of SiO_2-CaO-Al_2O_3 slag were utilized. For slag 1, a mixture of SiO_2, limestone and Al_2O_3 powder was melted in an induction furnace. The purity of the powders and the suppliers are presented in Table 2. To ensure a homogenous slag phase, the mixture was remelted three times up to 1800 °C, which is well above the expected liquidus temperature. Two slags from Kristiansen [21], slag 2 and 3, were also used. Table 3 presents the compositions of all three slags, along with their respective liquidus and solidus temperatures.

Table 2. The raw materials used for slag 1 and CaO for the dissolution experiments.

Product	Supplier	Purity
SiO_2	ThermoFisher Scientific (ThermoFisher, Trondheim, Norway) [22]	>99.9%
Limestone ($CaCO_3$)	Franzefoss Minerals AS (Franzefoss AS, Inderøy, Norway) [23]	>99.7%
Al_2O_3	ThermoFisher Scientific [22]	>99.9%

Table 3. SiO_2-CaO-Al_2O_3 slags used in the dissolution experiments. Slags 2 and 3 are from Kristiansen [21]. The amounts are given in wt%, the solidus and liquidus temperature are found from the SiO_2-CaO-Al2O3 ternary diagram [12] and the viscosities are calculated with FactSage 8.1. Λ^{corr} is the corrected optical basicity.

Slag	SiO_2 [wt%]	CaO [wt%]	Al_2O_3 [wt%]	$T_{liquidus}$ [°C]	$T_{solidus}$ [°C]	Λ^{corr}	Viscosity [Poise] 1500 °C	1550 °C
1	56	15	29	1490	1170	0.50	456	250
2	38	20	42	1550	1385	0.50	-	48
3	56	21	23	1420	1170	0.52	180	108

To prepare the CaO for the dissolution experiments, limestones purity from Franzefoss Minerals AS were heated in a muffle furnace at a heating rate of 5.6 °C/min up to 1000 °C. The limestones were then calcined for 1 h. The resulting CaO was then stored in a desiccator to prevent reactions with humidity or atmospheric CO_2 before the dissolution experiments.

The initial dissolution experiments were performed in a graphite tube furnace at 1600 °C. This furnace is equipped with a resistant graphite element for heat supply and the furnace temperature is controlled by a B-type thermocouple. Additionally, a C-type thermocouple is placed right above the sample. Samples containing 1 to 3 g of CaO and 25 to 30 g of slag 1 were heated with three different heating rates up to 1600 °C, which is well above the liquidus temperature of 1490 °C. Different holding times were used. The heating profiles are illustrated as the blue, green and grey lines in Figure 2.
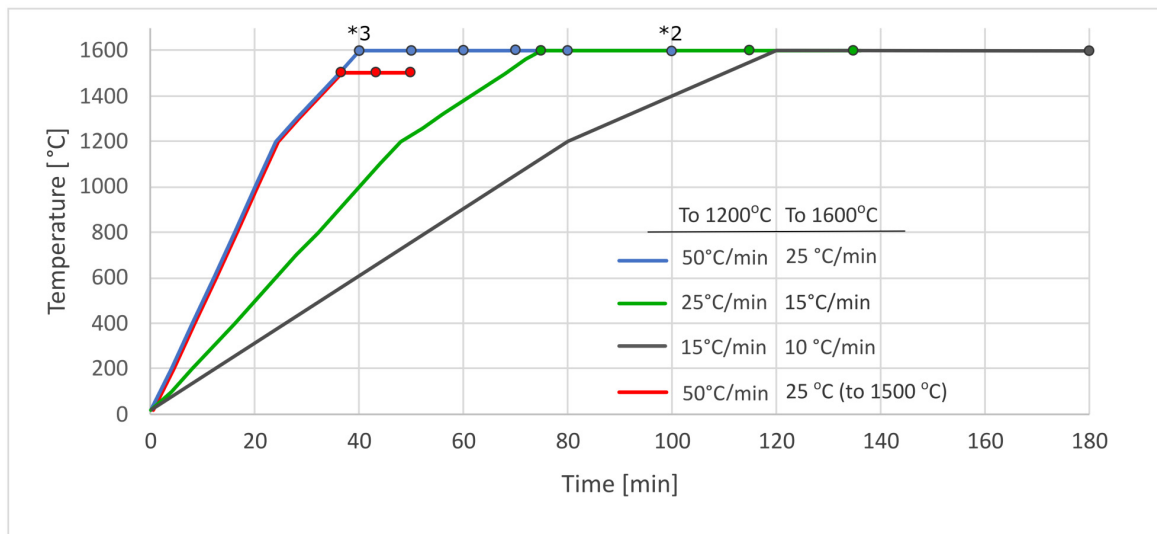
Figure 2. Heating profiles for the dissolution experiments in the graphite tube furnace shown as the blue, green and grey lines. The red line displays the heating profile for the sessile drop experiments at 1500 °C. The circles represent the different holding times, and "*2" and "*3" means that the experiment is repeated 2 and 3 times, respectively.

The next dissolution experiments were carried out in a sessile drop furnace for slag 1, 2 and 3 at 1500 °C and holding times of 0, 5 and 10 min. A 0 min holding time refers to no isothermal holding time. These are illustrated with the green line in Figure 2. A schematic overview of the sessile drop furnace can be seen in Figure 3. The sessile drop furnace has graphite heat elements, and the temperature is measured by a B-type thermocouple. For each experiment, approximately 0.2 to 0.3 g of slag and 0.04 to 0.07 g of CaO with physical contact were placed on a graphite substrate with 10 mm diameter and 3 mm height. Images of the slag and CaO before the experiment, and the slag after experiment can be seen in Figure 4.
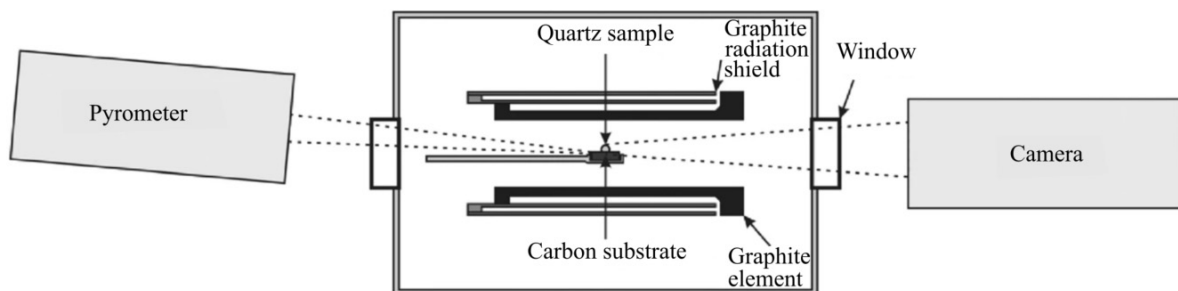
Figure 3. Schematic overview of the sessile drop furnace.
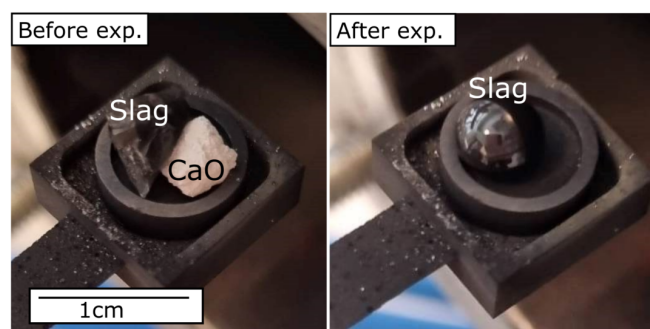
Figure 4. Slag and CaO before sessile drop experiment and slag after dissolution experiment.

Electron probe micro-analysis (EPMA), JEOL JXA 8500 (Japan Electron Optics Laboratory, Tokyo, Japan) was used to investigate the CaO and slag after both the graphite tube furnace experiments and the sessile drop furnace experiments. X-ray computed tomography (CT) was performed on some of the samples from the graphite tube furnace experiments to have a 3D view of the distribution of CaO in the SiO_2-CaO-Al_2O_3 slag. The scans were performed with a Nikon XT H 225 ST Instrument (NIKON Corporation, Tokyo, Japan). After the furnace experiments, the samples were first mounted in epoxy and then a vertical cross section was made in the middle of the samples. The cross-sections were imaged with EPMA, and to quantify the different elements in the samples, the oxide compositions were found using a wavelength-dispersive X-ray spectrometer (WDS).

3. Results and Discussion

3.1. CaO Dissolution in SiO_2-CaO-Al_2O_3 Slag

The dissolution of a CaO particle into a slag bath at 1600 °C during different holding times is illustrated in Figure 5. The initial CaO particle disintegrated between 1400 and 1500 °C and dissolved. The solidus temperatures for slag 1 and 3 are 1170 °C and 1385 °C for slag 2. This implies that the dissolution of CaO into the accumulated slag in Si furnaces may also occur if slag is present in the inactive zones, where the temperature exceeds the solidus temperature of the slag. At 1600 °C, there are CaO footprints in the slag. This was observed in the CT images, as shown in Figure 6. A brighter color, indicating a higher CaO content in the slag, accumulates at the bottom. Fractions with a higher concentration of CaO in the slag can also be observed higher up in the sample. From this, it appeared as the dissolution is very fast in the beginning before it slows down after around 20 min. This was also confirmed by the WDS analysis for the vertical samples, given in Figure 7.
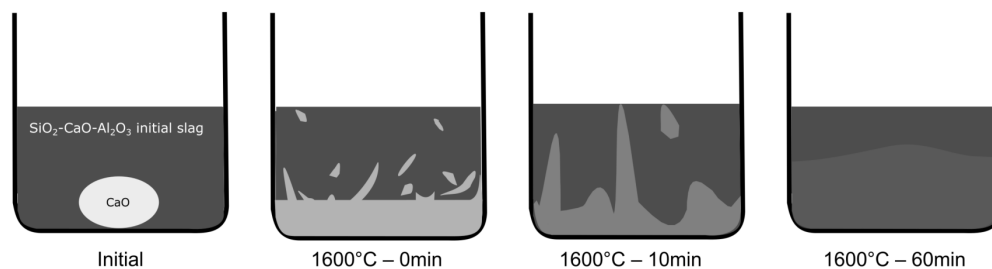
Figure 5. Schematic of the observed dissolution of a CaO particle into 56% SiO_2—15% CaO—29% Al_2O_3 at 1600 °C for different holding times in the graphite tube furnace.
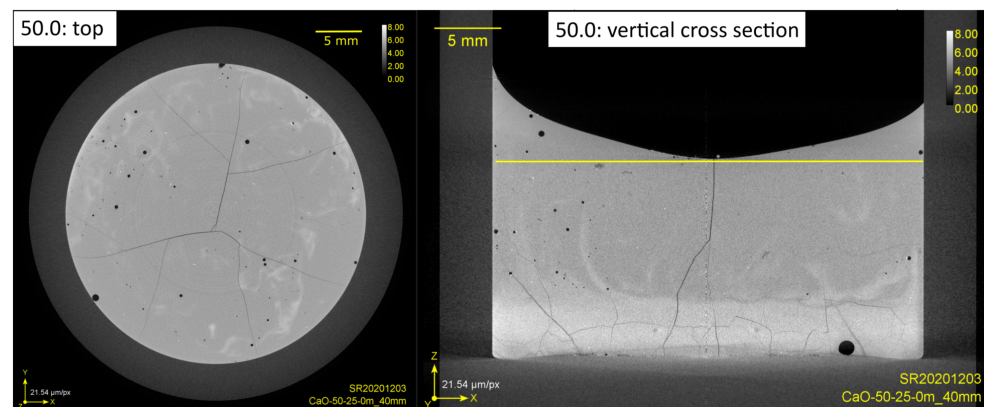
Figure 6. CT images from graphite tube furnace experiment of the second parallel heated to 1600 °C with heating rate 50 °C/min up to 1200 °C and 25 °C/min up to 1600 °C with 0 min holding time. To the left is an image from the top of the sample, and the right image is a vertical cross section in the center of the sample. The yellow line in the vertical section marks the height of the horizontal image. More CaO in the slag can be observed as the brighter grey color. The darkest grey color is the graphite crucible.
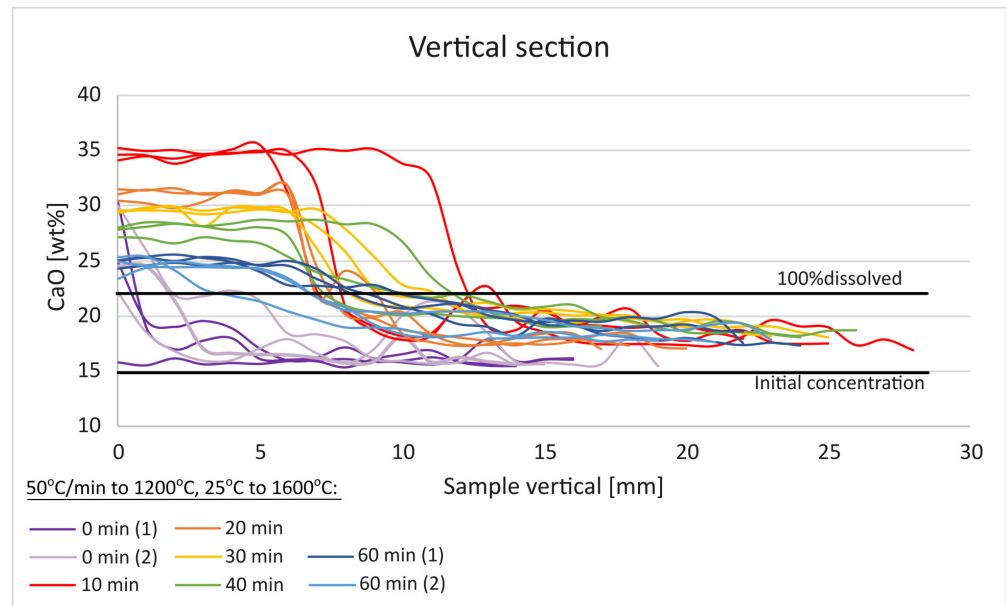
Figure 7. Results of WDS analysis vertical section for the samples with heating rate 50 °C/min to 1200 °C and 25 °C/min to 1600 °C. The CaO/slag ratio was 0.1.

3.2. Modeling the Dissolution Rate

For the dissolution experiments at 1500 °C, cross section images of the CaO and slag were captured using EPMA, and WDS analyses were performed from the CaO/slag interphase and across the slag. Images from three dissolution experiments with holding times of 0-, 5- and 10 min are presented in Figure 8. The red line represents the line analysis, and the results for slag 1, 2 and 3 can be found in Figure 9. The distance between each analysis points is 100 μm. It was observed a layer with brighter color around the CaO particle in the EPMA images. Previous research [24–27] has found a $2CaO \cdot SiO_2$ or $3CaO \cdot SiO_2$ layer next to the slag at the CaO–slag interface. However, in this study, the CaO concentration in these layers were from 35 to 42%, which is close to the 1500 °C liquidus line for slag 2 and somewhat lower than the $2CaO \cdot SiO_2$ phase boundary line. In this study, the layers are $CaO \cdot Al_2O_3 \cdot 2SiO_2$ for slag 1 and $2CaO \cdot Al_2O_3 \cdot SiO_2$ for slag 2 and 3.
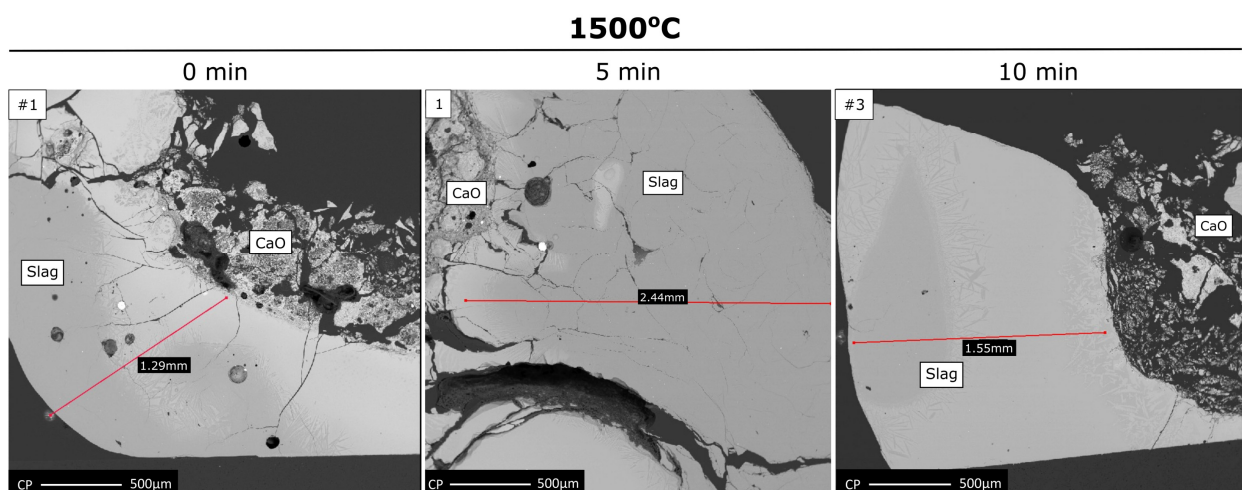
Figure 8. Cross section images and EPMA images after experiments for the 1500 °C experiments with CaO and slag 1 with 0, 5 and 10 min holding time.
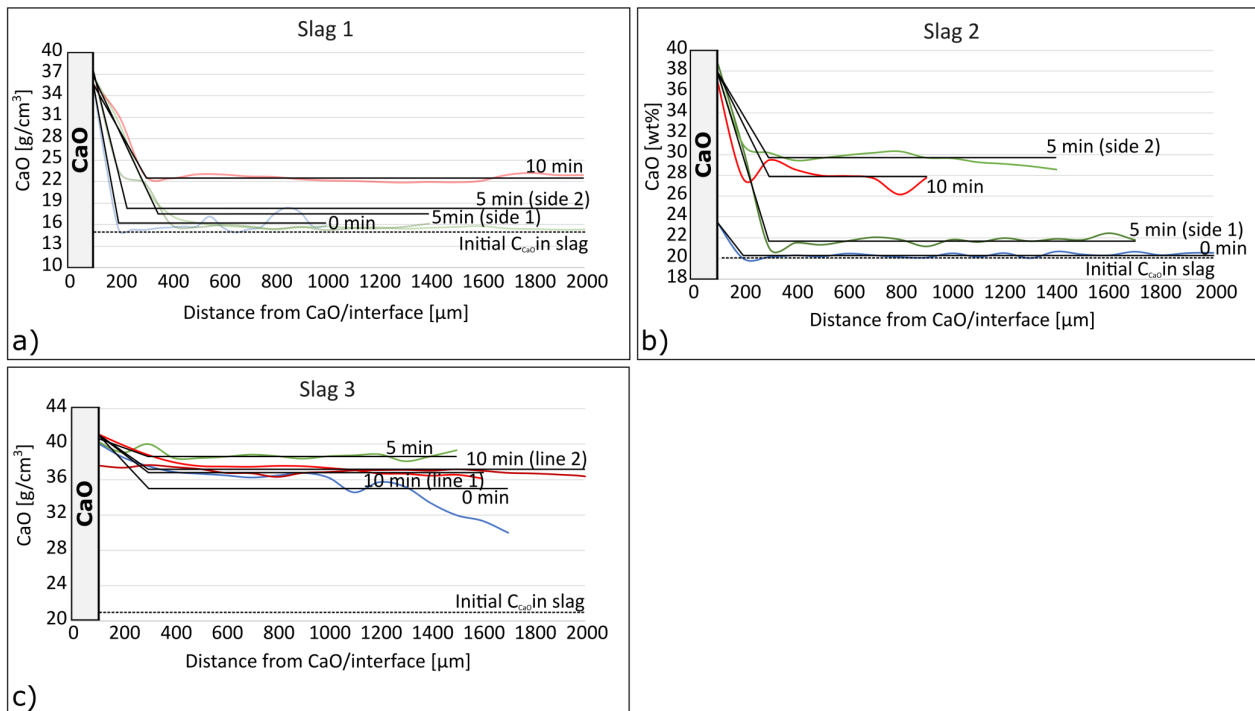
Figure 9. Dissolution curves for (**a**) slag 1, (**b**) slag 2 and (**c**) slag 3 for the experiments at 1500 °C with 0, 5 and 10 min holding time.

Two models for the dissolution of CaO in SiO_2-CaO-Al_2O_3 slag were used and compared with experimental results. The models are based on the experimental dissolution curves shown in Figure 9. The %CaO from outside the layer are the average slag concentrations, which are shown as the black, flat lines in the figures.

Theoretically, the reaction can be controlled by either the rate of the chemical reaction or mass transfer. In the first model, it is assumed that the dissolution is controlled by the rate of the chemical reaction. This is described by the shrinking sphere model [28,29], with the solid sphere CaO being consumed by dissolution into the liquid SiO_2-CaO-Al_2O_3 slag. The model assumes that the rate of reaction depends only on the surface area of the CaO. The rate of CaO dissolution in SiO_2-CaO-Al_2O_3 slag is proportional to its surface area, and the model assumes that mass transport is fast relative to the surface chemical reaction. The dissolution rate expression is then given by Equation (6) [29]:

$$R = \frac{dC}{dt}V = k_1 A_0 \left(1 - \frac{V}{M_0}\Delta C\right)^{\frac{2}{3}} \tag{6}$$

where R is the rate of dissolution, k_1 is the rate constant, and A_0 is the initial surface area of the total amount of CaO added, V is the volume of the slag, M_0 is the initial mass of added CaO. C is the CaO concentration in the slag at time t, and ΔC is defined as $\Delta C = C - C_i$.

The second model assumes that the rate is controlled by mass transport. This model, in addition to the rate constant and the surface area, considers the diffusion of dissolved CaO away from the solid CaO into the slag. The driving force for this diffusion is the concentration difference in dissolved CaO between that at the surface of the CaO, which is the saturated concentration, and that of the bulk of the SiO_2-CaO-Al_2O_3 slag. The dissolution rate can then be expressed, as shown in Equation (7) [28]:

$$R = \frac{dC}{dt}V = k_2 A(C_{sat} - C) = k_2 A_0 \left(1 - \frac{V}{M_0}\Delta C\right)^{\frac{2}{3}} (\Delta C_{sat} - \Delta C) \tag{7}$$

where k_2 is the rate constant, C_{sat} is the saturated/equilibrium concentration of CaO in the slag, and ΔC_{sat} is defined as $\Delta C_{sat} = C_{sat} - C_i$.

The modeled dissolution curves for slag 1, 2 and 3 together with the experimental results at 1500 °C can be seen in Figure 10. The rate data which were found to be the best fit from this model are listed in Table 4. The rate constants are in the order 10^{-5}–10^{-4} g/s·cm². Slag 3 is found to have the highest dissolution rate constant and slag 2 the lowest.
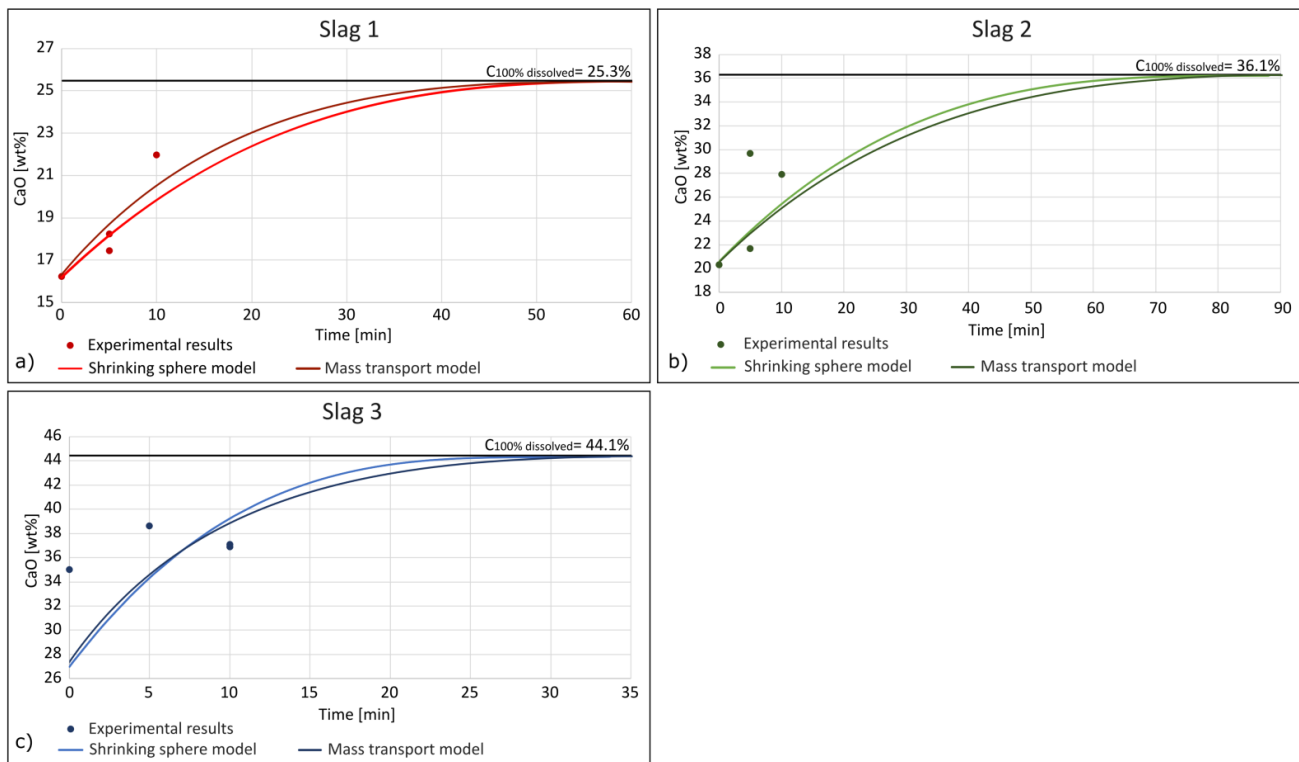
Figure 10. Modeled dissolution rate curves for (**a**) slag 1, (**b**) slag 2 and (**c**) slag 3 using shrinking sphere model and mass transport model. The curves are compared together with the experimental results.

Table 4. Rate data obtained from shrinking sphere model and mass transfer model. k_1 and k_2 are the rate constants and D is the diffusion coefficient.

Slag (SiO_2-CaO-Al_2O_3) [wt%]	Shrinking Sphere k_1 [g/s·cm²]	Mass Transport k_2 [cm/s]	D [cm²/s]
1: 56-15-29	1.2×10^{-4}	5.5×10^{-5}	1.7×10^{-6}
2: 38-20-42	9.0×10^{-5}	4.0×10^{-5}	1.2×10^{-6}
3: 56-21-23	2.9×10^{-4}	1.4×10^{-4}	4.2×10^{-6}

The dissolution of CaO in SiO_2-CaO-Al_2O_3 slag has been studied by a wide range of researchers, including [9,24–27,30–32], and it has been determined that mass transfer in the slag is the rate-determining step. Ions of Ca^{2+} and O^{2-} transfer through a $2CaO·SiO_2$ or $3CaO·SiO_2$ boundary layer next to slag at the CaO–slag interface. However, as the %CaO is not equal to the saturation CaO at the surface of the CaO particle, this is not the case in this study. Based on the experimental dissolution data presented in Figure 9, it is observed that the dissolution process in this study is a mix of chemical- and mass transfer-controlled reactions. Models based on either chemical or mass transfer control will therefore have some deviation from the actual dissolution rate curves. However, both models have similar curves for dissolution, and it is therefore assumed that the models are an acceptable approximation.

The diffusion coefficient, D, describes the amount of CaO that diffuses per time unit and can be found from relationship between the rate data and the boundary layer thickness, δ, through Equation (8) [28]. The boundary layer in this case is the $CaO \cdot Al_2O_3 \cdot 2SiO_2$ for slag 1 and $2CaO \cdot Al_2O_3 \cdot SiO_2$ for slag 2 and 3 layers, which is found outside the remaining CaO particle. The boundary layer thickness is assumed to be constant for all three slags.

$$k_2 = \frac{D}{\delta} \tag{8}$$

The diffusion constants for the three slag compositions are presented in Table 4, along with the rate data. The rate constants were found to be in the order of 10^{-6} cm^2/s, which is somewhat higher than the literature data for similar slags. Liang et al. [8] used the isotope tracer method and found the diffusion coefficients for a slag with composition of 65% SiO_2—20% CaO—15% Al_2O_3 to be 3.3×10^{-7} cm^2/s and for a composition of 60% SiO_2—20% CaO—20% Al_2O_3 to be 3.66×10^{-7} cm^2/s at 1500 °C. In the experiments in this study, the diffusion coefficient for slag 3, which has the most similar composition with 56% SiO_2—21% CaO—23% Al_2O_3, is found to be 5.7×10^{-6} cm^2/s. For the most studied slag composition of 40% SiO_2—40% CaO—20% Al_2O_3, the diffusion coefficients at 1500 °C are reported as 1.34×10^{-6} cm^2/s [8] and 2.6×10^{-6} cm^2/s [7]. The last case was calculated from the Nernst–Einstein relation. At lower temperatures, the diffusion coefficient was found to vary between 1.6×10^{-6}–1.3×10^{-7} cm^2/s [3–7,10]. This slag composition is on the same dissolution path as for slag 1, 56% SiO_2—15% CaO—29% Al_2O_3, where the diffusion coefficient was found to be in the same order, at 10^{-6} cm^2/s.

The diffusion coefficient is often found to be proportional with the viscosity, η, as derived from both Stokes–Einstein [12] and Eyring [13] equations for diffusivity. The calculated viscosities for slag 1, 2 and 3 at 1500 °C using FactSage 8.1 are 456 Poise, 82 Poise and 180 Poise, respectively. However, this model does not consider solid particles in the slag. The liquidus temperature of slag 2 is 1550 °C, which means that presence of solid particles in the melt at 1500 °C increases the viscosity considerably. It is therefore believed that slag 2 has the highest viscosity, and hence $\eta_{slag\ 2} > \eta_{slag\ 1} > \eta_{slag\ 3}$. This is consistent with $k_{slag\ 3} > k_{slag\ 1} > k_{slag\ 2}$.

3.3. The Effect of CaO on Slag Viscosity in Si Furnaces

The main purpose of adding CaO to Si furnaces is to lower the viscosity of the accumulated slag in the furnace. Too much accumulated slag is negative for the operation and a sufficient low viscosity is important to ensure a stable flow of materials through the furnace. However, with increasing amount of CaO added to the furnace, more SiO_2 will enter the slag phase. This gives less SiO_2 to react to Si and would hence decrease the Si yield. It is therefore beneficial to add the least amount of CaO that would decrease the slag viscosity sufficiently to have a stable flow of materials through the furnace. Accumulated slag analyzed from the higher, inactive parts of industrial furnaces have found CaO concentrations varying from ~10–30% [33], which are similar with the slag used in this study. The viscosities, as a function of increasing CaO concentration for the slags used in this study, can be seen in Figure 11. The initial CaO concentration for slag 1, 2 and 3 is 15%, 20% and 21%, respectively, and a great initial effect of dissolving more CaO into the slag systems can be observed. For slag 1 at 1600 °C, the viscosity decreases to 1/12 of its initial value when increasing the CaO concentration to 30%. From 30–35% CaO, the viscosity decrease is smaller. In the Si furnaces, the CaO is expected to disintegrate and dissolve in any slag close by. With increasing temperature, the dissolution rate also increases. The viscosity of the slag is therefore expected to decrease rapidly in contact with the CaO.
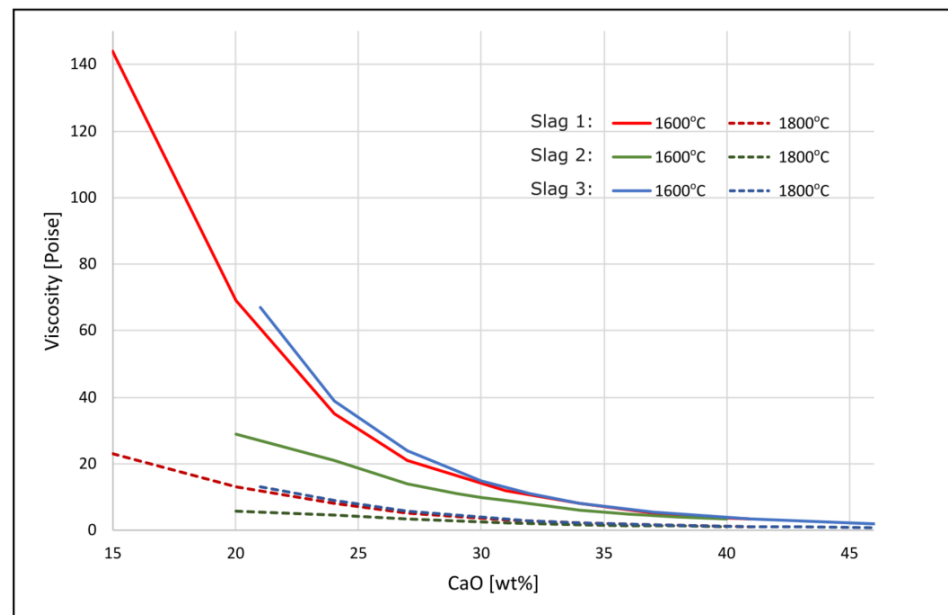
Figure 11. Viscosity with increasing %CaO for slag 1, 2 and 3 at temperature 1600 °C and 1800 °C. The viscosities are calculated using FactSage 8.1.

4. Conclusions

Increased knowledge on how CaO dissolves into different SiO_2-CaO-Al_2O_3 slags relevant for the Si production is important to know the effect of adding limestone together with the raw materials. Addition of limestone is the main action used today for reducing the viscosity of the slag and thereby prevent accumulation. The dissolution and the dissolution rate of CaO into three different compositions of slags with CaO content of 15–21% were investigated through experiments up to 1600 °C. The main observation is that the dissolution is fast, and that the dissolution starts during heating at around 1300–1400 °C, which means that the dissolution starts in the higher parts in the Si furnaces.

- Initial CaO disintegrates during heating before it dissolves in the slag. During the dissolution process, a layer with 35–42% CaO is formed between the CaO particle and the slag, which for slag 1 correspond to $CaO·Al_2O_3·2SiO_2$, and $2CaO·Al_2O_3·SiO_2$ for slag 2 and 3. This is different from earlier research [24–27], which has found a $2CaO·SiO_2$ or $3CaO·SiO_2$ layer next to the slag at the CaO–slag interface.
- Two models for the dissolution rate for the three slags in this study were made. In the first model, the CaO particle is assumed to be a smooth shrinking sphere, and the rate controlled by the rate of chemical reaction. The second model assumes that the rate is controlled by the mass transport and depends on the diffusion rate of CaO through a boundary layer at the surface of the CaO. In both models, it was found that $k_{slag\,3} > k_{slag\,1} > k_{slag\,2}$, which is consistent with proportional relationship with viscosities. The diffusion coefficients are found to be in the range of 10^{-6} cm^2/s.
- The initial effect of increasing the CaO content in the slag from 15–21% to 25–30% gives a significant reduction in the viscosity.

Author Contributions: Conceptualization, M.B.F. and M.T.; methodology, M.B.F. and K.E.E.; software, M.B.F.; validation, M.B.F., K.E.E. and M.T.; data curation, M.B.F.; writing—original draft preparation, M.B.F.; writing—review and editing, M.B.F., K.E.E. and M.T.; supervision, K.E.E. and M.T.; All authors have read and agreed to the published version of the manuscript.

Data Availability Statement: The data presented in this study is available on request from the corresponding author. The data are not publicly available due to privacy reasons.

Conflicts of Interest: The authors declare no conflicts of interest.

References

1. Schei, A.; Tuset, J.K.; Tveit, H. *Production of High Silicon Alloy*; Tapir: Trondheim, Norway, 1998; pp. 47–72.
2. Myrhaug, E. KPN CONTROLLED TAPPING, Examples of conceptual models based on simplified COMSOL simulations. In Proceedings of the Industrial presentation from Elkem ASA, KPN Controlled Tapping Meeting 2020.03.05 regarding Conceptual Models, NTNU, Trondheim, Norway, 5 April 2020.
3. Towers, H.; Paris, M.; Chipman, J. Diffusion of Calcium Ion in Liquid Slag. *JOM* **1953**, *5*, 1455–1458. [CrossRef]
4. Towers, H.; Chipman, J. Diffusion of Calcium and Silicon in a Lime-Alumina-Silica Slag. *JOM* **1957**, *9*, 769–773. [CrossRef]
5. Niwa, K. A study on the Diffusion of Calcium Ion in Molten Lime-Silica-Alumina slags by Using a Radioactive Tracer Technique. *J. Jpn. Inst. Met. Mater.* **1957**, *21*, 304–308. [CrossRef]
6. Saitô, T.; Maruya, K. Diffusion of Calcium in Liquid Slags. *Res. Inst. Miner. Dress. Metall.* **1958**, *10*, 306–314.
7. Goto, K.S.; Sasabe, M.; Kawakami, M. Relation between Tracer Diffusivity and Electrical Conductivity on Multi-component Oxide Slags at 900 ° to 1600 °C. *Trans. Iron Steel Inst. Jpn.* **1977**, *17*, 212–214. [CrossRef]
8. Liang, Y.; Richter, F.M.; Davis, A.M.; Watson, B.E. Diffusion in silicate melts: I. Self diffusion in CaO-Al$_2$O$_3$-SiO$_2$ at 1500 °C and 1 GPa. *Geochim. Cosmochim. Acta* **1996**, *60*, 4353–4367. [CrossRef]
9. Amini, S.H.; Brungs, M.P.; Ostrovski, O.; Jahanshani, S. Effects of additives and temperature on dissolution rate and diffusivity of lime in Al$_2$O$_3$-CaO-SiO$_2$ based slags. *Metall. Mater. Trans. B* **2006**, *37*, 773–780. [CrossRef]
10. Zhang, G.; Chou, K. Diffusion Coefficient of Calcium Ion in CaO-Al$_2$O$_3$-SiO$_2$ Melts. *J. Iron Steel Res.* **2011**, *18*, 13–16. [CrossRef]
11. Ren, Z.S.; Hu, X.H.; Chou, K.C. Model for diffusion coefficient estimation of calcium ions in CaO–Al$_2$O$_3$–SiO$_2$ slags. *Ironmak. Steelmak.* **2013**, *40*, 625–629. [CrossRef]
12. Verein Deutscher Eisenhüttenleute. *Slag Atlas*; Stahlinstitut VDEh: Düsseldorf, Germany, 1995; pp. 105–545.
13. Glasstone, S.; Laidler, K.J.; Eyring, H. *The Theory of Rate Processes: The Kinetics of Chemical Reactions, Viscosity, Diffusion and Electrochemical Phenomena*; McGraw-Hill Book Company: New York, NY, USA, 1941; pp. 516–523.
14. Hofmann, A.W. Diffusion in natural silicate melts: A critical review. In *Physics of Magmatic Processes*; Princeton University Press: Princeton, NJ, USA, 1980; pp. 385–417.
15. Angell, C.A.; Cheeseman, P.A.; Tamaddon, S. Pressure Enhancement of Ion Mobilities in Liquid Silicates from Computer Simulation Studies to 800 Kilobars. *Science* **1982**, *218*, 885–887. [CrossRef]
16. Watson, E.B. Calcium diffusion in a simple silicate melt to 30 kbar. *Geochim. Cosmochim. Acta* **1979**, *43*, 313–322. [CrossRef]
17. Dogan, N.; Brooks, G.A.; Rhamdhani, M.A. Kinetics of Flux Dissolution in Oxygen Steelmaking. *ISIJ Int.* **2009**, *49*, 1474–1482. [CrossRef]
18. Mills, K.C.; Sridhar, S. Viscosities of ironmaking and steelmaking slags. *Ironmak. Steelmak.* **1999**, *26*, 262–268. [CrossRef]
19. Folstad, M.B.; Tangstad, M. SiO$_2$-CaO-Al$_2$O$_3$ slags in the Si/FeSi furnaces. In Proceedings of the 16th International Ferro-Alloys Congress (INFACON XVI) 2021, Trondheim, Norway, 28–29 September 2021.
20. Jusnes, K.F.; Hjelmseth, R.; Folstad, M.B.; Ditlefsen, N.S.; Tangstad, M. Investigation of slag compositions and possible relation to furnace operation of a FeSi75 furnace. In Proceedings of the 16th International Ferro-Alloys Congress (INFACON XVI) 2021, Trondheim, Norway, 28–29 September 2021.
21. Kristiansen, S. Dissolution Rate and Wettability of SiO$_2$–CaO–Al$_2$O$_3$ Slag on Quartz. Project Work. Master's Thesis, Norwegian University of Science and Technology, Department of Materials Science and Engineering, Trondheim, Norway, 2022.
22. ThermoFisher Scientific. Available online: https://www.thermofisher.com/no/en/home.html (accessed on 8 January 2024).
23. Franzefoss Minerals AS. Available online: https://kalk.no/en/ (accessed on 8 January 2024).
24. Amini, S.; Brungs, M.; Ostrovski, O. Dissolution of Dense Lime in Molten Slags under Static Conditions. *ISIJ Int.* **2007**, *47*, 32–37. [CrossRef]
25. Sato, D.; Kubota, R.; Nishimoto, A.; Kubota, M.; Matsuda, H. Kinetic Study on Dissolution of CaO Particle into CaO-SiO$_2$-Al$_2$O$_3$ Molten Slag from Simulated Municipal Solid Wastes Melting. *J. Chem. Eng. Jpn.* **2017**, *50*, 324–331. [CrossRef]
26. Kimura, H.; Yanagase, T.; Noguchi, F.; Ueda, Y. Studies on the Mechanism of CaO Dissolution into Slag Melts. *J. Jpn. Inst. Met.* **1974**, *38*, 226–232. [CrossRef]
27. Cooper, A.R., Jr.; Kingery, W.D. Dissolution in Ceramic Systems: I, Molecular Diffusion, Natural Convection, and Forced Convection Studies of Sapphire Dissolution in Calcium Aluminum Silicate. *J. Am. Ceram. Soc.* **1964**, *47*, 37–43. [CrossRef]
28. Haverkamp, R.G.; Welch, B.J.; Metson, J.B. Models of Alumina Dissolution in Cryolite. *ECS Proc. Vol.* **1992**, *1996-16*, 646–659. [CrossRef]
29. Marabi, A.; Mayor, G.; Burbidge, A.; Wallach, R.; Saguy, I.S. Assessing dissolution kinetics of powders by a single particle approach. *Chem. Eng. J.* **2008**, *139*, 118–127. [CrossRef]
30. Matsushima, M.; Yadoomaru, S.; Mori, K.; Kawai, Y. A Fundamental Study on the Dissolution Rate of Solid Lime into Liquid Slag. *Trans. Iron Steel Inst. Jpn.* **1977**, *17*, 442–449. [CrossRef]
31. Kitamura, S. Dissolution Behavior of Lime into Steelmaking Slag. *ISIJ Int.* **2017**, *57*, 1670–1676. [CrossRef]

32. Guo, X.; Sun, Z.H.I.; Van Dyck, J.; Guo, M.; Blanpain, B. In Situ Observation on Lime Dissolution in Molten Metallurgical Slags–Kinetic Aspects. *Ind. Eng. Chem. Res.* **2014**, *53*, 6325–6333. [CrossRef]
33. Folstad, M. Slag and Its Effect on Si and FeSi Production. Ph.D. Thesis, Norwegian University of Science and Technology, Trondheim, Norway, 2023. Available online: https://hdl.handle.net/11250/3096091 (accessed on 8 January 2024).